

# Continuously tunable SIW phase shifter based on the buried varactors

Hao Peng<sup>1a)</sup>, Peng Jiang<sup>1</sup>, Tao Yang<sup>1</sup>, and Haiyan JIN<sup>2</sup>

<sup>1</sup> School of Electronic Engineering, University of Electronic Science and Technology of China, No.2006, Xiyuan Ave, West Hi-Tech Zone, Chengdu, 611731, China

<sup>2</sup> School of Communication and Information Engineering,  
University of Electronic Science and Technology of China,  
No. 4, Section 2, North Jianshe Road, Chengdu, 610054, China  
a) [ph1984.1.25@163.com](mailto:ph1984.1.25@163.com)

**Abstract:** A continuously tunable substrate integrated waveguide (SIW) phase shifter based on the buried varactors is proposed. A number of varactors buried within the substrate are introduced into the SIW section. Varactor diode is a nonlinear device, of which the capacitance varies with applied voltage of an exponent factor negative fractional value. The distribution of electric and magnetic fields can be changed with varied capacitance, which results in the phase-shifted. As one example, a phase shifter with four varactors is designed and implemented. Simulation and experimental results are in good agreements. The measured results show a return loss mostly better than 10 dB and an insertion loss less than 2.3 dB within a frequency range from 1.6 to 2.6 GHz (about 47.6% relative bandwidth). The maximum phase range is about 30° at the center frequency.

**Keywords:** SIW, phase shifter, buried varactors

**Classification:** Microwave and millimeter wave devices, circuits, and systems

## References

- [1] M. Bozzi, A. Georgiadis and K. Wu: IET Microw. Antennas Propag. **5** (2011) 909. DOI:10.1049/iet-map.2010.0463
- [2] Y. J. Cheng, W. Hong and K. Wu: IEEE Trans. Microw. Theory Techn. **58** (2010) 203. DOI:10.1109/TMTT.2009.2035942
- [3] O. Kramer, T. Djerafi and K. Wu: IET Microw. Antennas Propag. **6** (2012) 1704. DOI:10.1049/iet-map.2012.0272
- [4] K. Sellal, L. Talbi, T. A. Denidni and J. Lebel: IET Microw. Antennas Propag. **2** (2008) 194. DOI:10.1049/iet-map:20070135
- [5] T. Yang, M. Ettorre and R. Sauleau: IEEE Microw. Wireless Compon. Lett. **22** (2012) 518. DOI:10.1109/LMWC.2012.2217122
- [6] M. Ebrahimpouri, S. Nikmehr and A. Pourziad: IEEE Microw. Wireless Compon. Lett. **24** (2014) 748. DOI:10.1109/LMWC.2014.2350692
- [7] K. Sellal, L. Talbi and M. Nedil: IET Microw. Antennas Propag. **6** (2012) 1090. DOI:10.1049/iet-map.2011.0380
- [8] F. Yang, H. X. Yu, B. Zhang, Y. Zhou and Z. X. Zhu: ICECC (2011) 3966.
- [9] Y. Ding and K. Wu: IEEE MTT-S International (2012) 1. DOI:10.1109/

- MWSYM.2012.6259459
- [10] Y. Ding and K. Wu: IEEE MTT-S International (2011) 1. DOI:10.1109/MWSYM.2012.6259459
- [11] E. Sbarra, L. Marcaccioli, R. Vincenti and R. Sorrentino: EuMC (2009) 264.

## 1 Introduction

Phase shifter is an important component in microwave and millimeter-wave circuits and systems. It has been widely used in phase array antenna, wireless communication system, test instrument, signal modulation and demodulation, and other application systems. In recent years, substrate integrated waveguide (SIW) technique as one kind of novel electromagnetic wave propagation structure has been paid attention to by more and more researchers. The structure of SIW, which can offer the advantages of low insertion loss, high quality factor, low electromagnetic radiation, high power capacity and easy integration with the microstrip line or coplanar line, is constructed by metallic-vias in the dielectric substrate [1]. Various types of SIW phase shifters, which have been reported correspondingly in the past decade, are primarily divided into two categories: fixed phase shifter [2, 3, 4, 5, 6] and electronic tunable phase shifter. The latter can be further divided as digital phase shifter [7] and analog phase shifter [8, 9, 10, 11]. There are some limitations for the mentioned phase shifters above. The fixed one has a disadvantage of inflexibility for phase-shifted, and the RF switch is ordinarily needed to be incorporated into the circuit. For the digital one, some certain phase degrees may be missed. It should be noted that all of the previously reported analog phase shifters [8, 9, 10, 11] consist of couplers as a key component. The circuit structure for analog phase shifters becomes more complex. To overcome these problems, the analog SIW phase shifter is introduced.

In this letter, a continuously tunable SIW phase shifter based on four varactors, which buried within the substrate, is presented. The function of phase shifting can be achieved with the SIW load fluctuation. To prove this idea, a continuously tunable SIW phase shifter is designed, fabricated and measured. The measured results show good agreement with the simulated ones. A return loss better than 10 dB and an insertion loss less than 1 dB within a frequency range from 1.8 to 2.8 GHz are obtained. In the next sections, the principle of SIW phase shifter, the circuit model and the results will be presented and discussed.

## 2 Theoretical analysis

A cylindrical metal post, which is inserted in the SIW structure, is equivalent to a T-network and a phase shifter [4]. In the equivalent circuit of Fig. 1, the capacitive coupling effect between the metal sides of the SIW and the cylindrical metal post is represented by two capacities while the mutual coupling effect between the top and bottom metal conductors is represented by an inductance. The relationship between the phase  $\phi$  and the normalized reactance  $X$ , the normalized susceptance  $B$  is given below as Eq. (1).

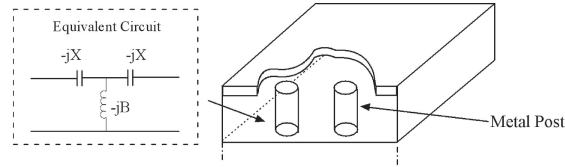


**Fig. 1.** Equivalent circuit model of metal post inserted in SIW.

$$\phi = \tan^{-1} \left[ \frac{B + 2X - BX^2}{2(1 - BX)} \right] \quad (1)$$

As mentioned in [7], a controllable digital phase shifter in SIW is designed and implemented. A PIN diode, buried within SIW, will show the similar electrical characteristics as the metal post. If the varactors, capacitance of which is varied with the control voltage, are placed in SIW structure in a certain order, a discrete digital phase shifter maybe turn into a continuous analog phase shifter.

Next, the principle of continuously tunable phase shifter, based on the buried varactor, will be analysed in detail. A varactor, inserted in the SIW, is equivalent to a T-network in Fig. 2. A weak series resistance  $R_s$  of the varactor equivalent circuit is neglected. The normalized reactance  $1/Y$  and the normalized susceptance  $D$  respectively represent the capacitive coupling effect between the metal sides of the SIW and varactor and the variable capacitance  $C_j$  of varactor.

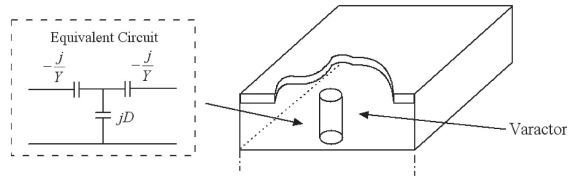


**Fig. 2.** Equivalent circuit model of a varactor inserted in SIW.

Two or more two-port networks can be easily defined by multiplying the transmission (ABCD) matrix of the individual two-ports. The transmission matrix of this model in Fig. 2 can be expressed as follow:

$$\begin{pmatrix} a & b \\ c & d \end{pmatrix} = \begin{bmatrix} 1 & -j/Y \\ 0 & 1 \end{bmatrix} \begin{bmatrix} 1 & 0 \\ jD & 1 \end{bmatrix} \begin{bmatrix} 1 & -j/Y \\ 0 & 1 \end{bmatrix} = \begin{bmatrix} 1 + \frac{D}{Y} & \frac{2}{jY} + \frac{D}{jY^2} \\ jD & 1 + \frac{D}{Y} \end{bmatrix} \quad (2)$$

The conversion for two-port network parameters between scattering matrix and transmission matrix is given below:

$$S_{21} = \frac{2}{a + b + c + d} = 2 \left[ 2 \left( 1 + \frac{D}{Y} \right) - j \left( D - \frac{2}{Y} - \frac{D}{Y^2} \right) \right] / \Delta \quad (3)$$

Where

$$\Delta = 4 \left( 1 + \frac{D}{Y} \right)^2 + \left( D - \frac{2}{Y} - \frac{D}{Y^2} \right)^2 \quad (4)$$

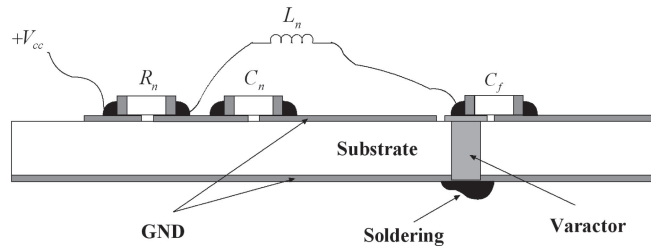
Therefore, the phase shift  $\theta$  can be written in the following form:

$$\theta = \tan^{-1} \left[ \left( -Y + \frac{2}{D} + \frac{1}{Y} \right) / 2 * \left( \frac{Y}{D} + 1 \right) \right] \quad (5)$$

For a given SIW structure in a certain frequency, the value  $Y$  is a constant. The phase shift  $\theta$  varies with the variable capacitance value  $D$  of varactor in Eq. (5).

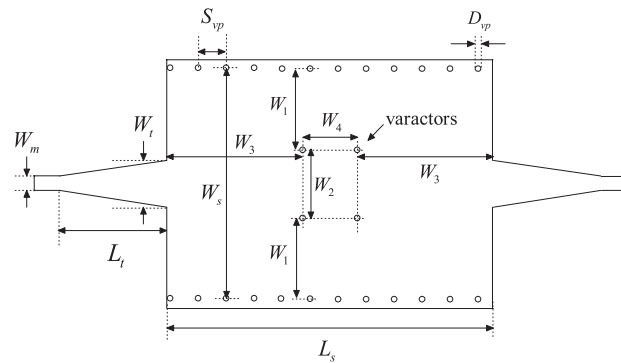
For the purpose of easy installation, the shape of the cylindrical structure for varactors is selected. Thus, in this study, the varactor (Model: 2B11B), manufactured by the Chengdu Yaguang Electronic Limited by Share Ltd, is chose for its weak series resistance  $R_s$  (less than  $1\ \Omega$ ) and a typical variable capacitance range from 0.23 pF to 1.46 pF (from 30 V to 0 V). In addition, the dimensions of cylindrical varactors, inserted inside the non-metallic holes, are listed below: 1.29 mm in diameter and 1.42 mm in length.

Fig. 3 shows the biasing circuit of a varactor. One terminal of the varactor is soldered to GND, and the other terminal is connected with a power supply. Note that the capacitance of  $C_f$  is a fixed value (1 nF), the inductance of  $L_n$  is 100 nH, the capacitance of  $C_n$  is 1 nF, and the resistance of  $R_n$  is 1 K $\Omega$ .  $R_n$ ,  $L_n$  and  $C_n$  are used as a power filtering network, and the  $C_f$  is used as a microwave signal path to GND. With the variation of the DC voltage, the capacitance of varactor will be changed.



**Fig. 3.** Biasing circuit of a varactor.

In the light of the preceding statement, a continuously tunable SIW phase shifter is shown in Fig. 4. SIW phase shifter consists of four parts, which are two microstrip lines, two microstrip-to-SIW transitions, a SIW section and four varactors buried within the substrate.



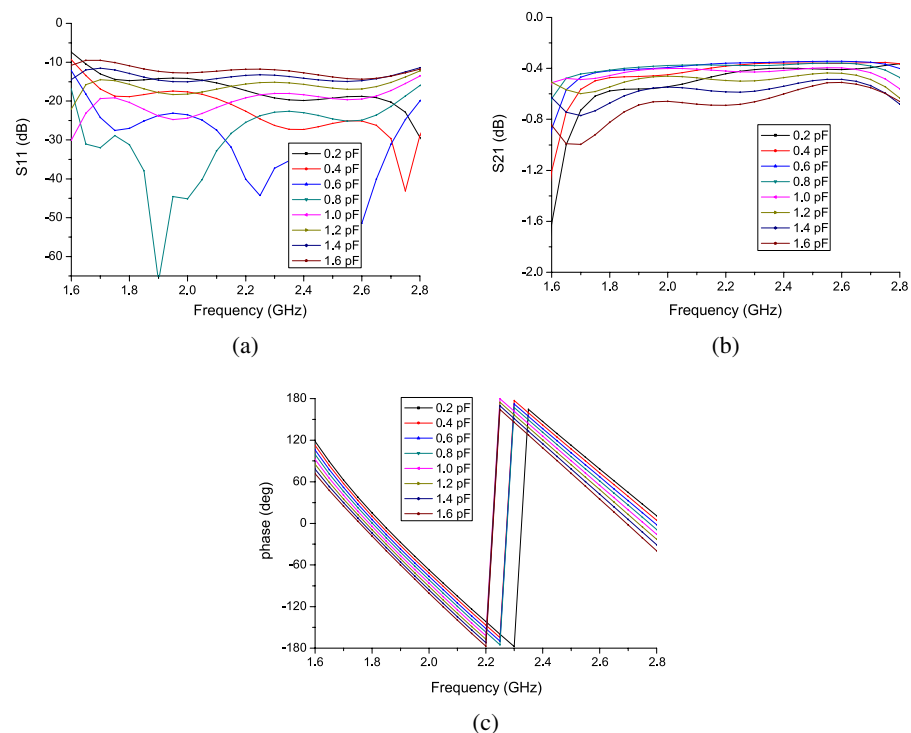
**Fig. 4.** View of the continuously tunable SIW phase shifter.

The diameter of the non-metallic holes is slightly bigger than the diameter of the varactors. ROGERS RT/Duroid 4003 substrate, with relative dielectric constant of 3.38, loss tangent of 0.0027 and thickness of 1.524 mm, is selected. The key dimensions of the phase shifter are determined to be  $W_m = 3.409$  mm,  $W_t = 10$  mm,  $L_t = 23$  mm,  $S_{vp} = 1.6$  mm,  $D_{vp} = 0.8$  mm,  $W_s = 50.432$  mm,  $L_s = 70$  mm,  $W_1 = 29.1$  mm,  $W_2 = 11.8$  mm,  $W_3 = 17.915$  mm,  $W_4 = 14.6$  mm.

### 3 Simulation and measurement

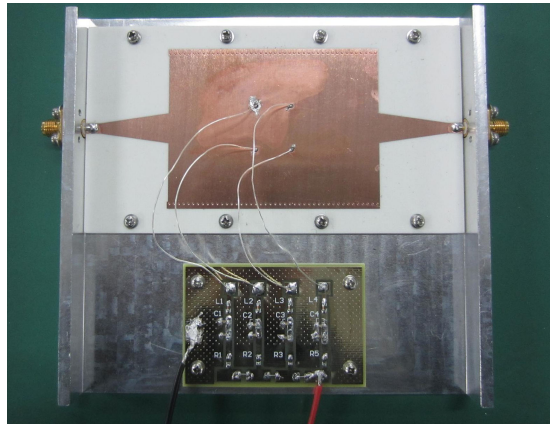
To confirm our previous idea, a commercial CAD tool (High Frequency Structure Simulator, HFSS) is applied to carry out the full-wave simulation method. Moreover, the complete simulation model of the varactor does not exist in HFSS. The varactor model can be defined as a rectangle RLC boundary.

Fig. 5 shows the simulation results of the proposed phase shifter in this letter. In the frequency range from 1.8 to 2.8 GHz, the return loss is better than 10 dB, the insertion loss is less than 1 dB, and the phase differences are respectively  $34.6^\circ$  and  $36.6^\circ$  at the frequency points of 2.1 GHz and 2.3 GHz. Therefore, the simulation results correspond to a variable capacitance range from 0.2 pF to 1.6 pF. Seen from these simulation results, the continuously tunable phase shifter operation in SIW can be achieved based on the buried varactors.



**Fig. 5.** Simulation results (a) Return loss (b) Insertion loss (c) Phase.

The relationship between bias voltage and capacitance is nonlinear. Some of the key and special voltage levels, which substantially corresponds to the same step capacitance for the varactor, are selected such as 0 V, 0.2 V, 0.4 V, 1.2 V, 2.2 V, 5 V, 13 V and 30 V. A photograph of fabricated phase shifter is shown in the Fig. 6. The bypass capacitor  $C_f$  is packaged in SMD 0402 package (1.0 mm \* 0.5 mm).



**Fig. 6.** Photograph of fabricated phase shifter.

Fig. 7 shows the measured results of the phase shifter. In the frequency range from 1.6 to 2.6 GHz, the return loss is mostly better than 10 dB, the insertion loss is less than 2.3 dB, and the phase differences are respectively  $30^\circ$  and  $32.3^\circ$  at the frequency points of 2.1 GHz and 2.3 GHz. Compared with the simulation and measured results, the return loss and the phase are in a good agreement between simulation and measurement. The measured insertion loss is slightly larger than the simulation in high frequency due to assembly error, SMA connectors, ideal circuit model neglected the varactor configuration, inconsistency of varactors and wires for power supply.

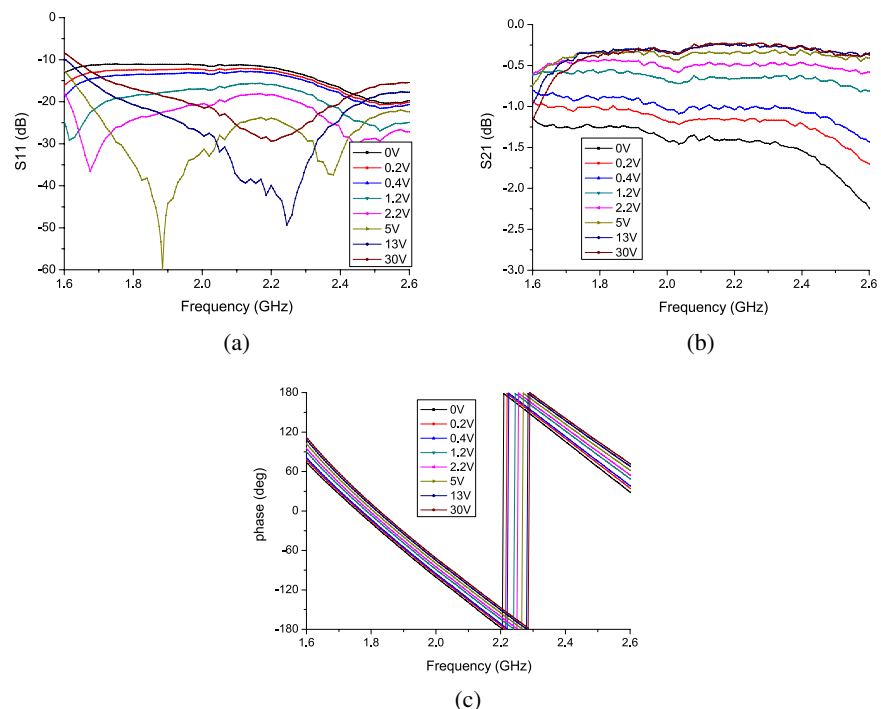


**Fig. 7.** Measured results (a) Return loss (b) Insertion loss (c) Phase.

There is another conclusion drawn from Table I. These data can clearly prove the correctness of design method. Table II gives a comparison between our study and some other SIW phase shifters reported by other researchers. As can be seen, the proposed phase shifter has the advantages of a large relative bandwidth

(47.6%), a simple realization method and the continuous phase change. The maximum phase range of this phase shift circuit is approximately 30°.

**Table I.** Simulated and measured datas at 2.1 GHz and 2.3 GHz

Freq, GHz	Voltage	Capacitance	S11, dB Sim.	Meas.	S21, dB Sim.	Meas.	Phase, ° Sim.	Meas.
2.1	0.05 V	1.4 pF	−14.2	−11.3	−0.56	−1.31	0	0
2.1	0.4 V	1.2 pF	−16.9	−12.9	−0.47	−1.03	4.9	5.5
2.1	1.2 V	1 pF	−21.7	−15.9	−0.41	−0.67	9.9	12.1
2.1	2.2 V	0.8 pF	−32.8	−18.7	−0.37	−0.49	15	16
2.1	5 V	0.6 pF	−27.5	−25.6	−0.37	−0.35	19.9	21.2
2.1	13 V	0.4 pF	−19.3	−37.6	−0.42	−0.27	25	25.9
2.1	30 V	0.2 pF	−15.3	−25.6	−0.5	−0.26	29.8	29.2
2.3	0.05 V	1.4 pF	−13.4	−13.8	−0.58	−1.35	0	0
2.3	0.4 V	1.2 pF	−15.2	−15.1	−0.5	−1.03	5.3	6.8
2.3	1.2 V	1 pF	−18	−18	−0.43	−0.65	10.5	14.3
2.3	2.2 V	0.8 pF	−22.9	−21	−0.38	−0.48	15.8	18.5
2.3	5 V	0.6 pF	−37.3	−28.2	−0.35	−0.34	20.9	24.1
2.3	13 V	0.4 pF	−26.3	−35.6	−0.36	−0.27	26.2	29
2.3	30 V	0.2 pF	−19.2	−25.3	−0.41	−0.26	31.2	32.3

**Table II.** Comparison between the SIW phase shifters

	Maximum phase range	Relative bandwidth	Analog/Digital/Fixed	Difficulty degree
This letter	30°	47.6%	Analog	Simple
Ref. [2]	45°/90°	50%	Fixed	Simple
Ref. [5]	60°	12.5%	Fixed	Medium
Ref. [7]	45°	10%	Digital	Simple
Ref. [8]	360°	11.5%	Analog	Difficulty
Ref. [9]	360°	12%	Analog	Difficulty
Ref. [10]	180°	11.8%	Analog	Difficulty

#### 4 Conclusion

In this letter, a novel continuously tunable SIW phase shifter, based on the varactors buried within SIW section, has been demonstrated. This analog phase shifter is indirectly and directly controlled by the DC voltage and the change of capacitance. A modular of phase shifter is designed, manufactured and measured. Simulation and experimental results are in good agreements.

#### Acknowledgments

This work was supported by the China Postdoctoral Science Foundation under Grant 2014M552337.